



CHALMERS

Chalmers Publication Library

Nanocomposites of polyacrylic acid nanogels and biodegradable polyhydroxybutyrate for bone regeneration and drug delivery

This document has been downloaded from Chalmers Publication Library (CPL). It is the author's version of a work that was accepted for publication in:

Journal of Nanomaterials (ISSN: 1687-4110)

Citation for the published paper:

Larsson, M. ; Bergstrand, A. ; Mesiah, L. (2014) "Nanocomposites of polyacrylic acid nanogels and biodegradable polyhydroxybutyrate for bone regeneration and drug delivery". Journal of Nanomaterials, vol. 2014 pp. Article ID: 371307.

<http://dx.doi.org/10.1155/2014/371307>

Downloaded from: <http://publications.lib.chalmers.se/publication/192430>

Notice: Changes introduced as a result of publishing processes such as copy-editing and formatting may not be reflected in this document. For a definitive version of this work, please refer to the published source. Please note that access to the published version might require a subscription.

Chalmers Publication Library (CPL) offers the possibility of retrieving research publications produced at Chalmers University of Technology. It covers all types of publications: articles, dissertations, licentiate theses, masters theses, conference papers, reports etc. Since 2006 it is the official tool for Chalmers official publication statistics. To ensure that Chalmers research results are disseminated as widely as possible, an Open Access Policy has been adopted. The CPL service is administrated and maintained by Chalmers Library.

(article starts on next page)

Research Article

Nanocomposites of Polyacrylic Acid Nanogels and Biodegradable Polyhydroxybutyrate for Bone Regeneration and Drug Delivery

Mikael Larsson,^{1,2,3} Anna Bergstrand,^{1,3} Lilyan Mesiah,¹
Celine Van Vooren,¹ and Anette Larsson^{1,3}

¹ Department of Chemical and Biological Engineering, Chalmers University of Technology, 41296 Gothenburg, Sweden

² Ian Wark Research Institute, University of South Australia, Mawson Lakes Campus, Mawson Lakes, SA 5095, Australia

³ SuMo BIOMATERIALS, VINN Excellence Center at Chalmers University of Technology, 41296 Gothenburg, Sweden

Correspondence should be addressed to Mikael Larsson; larsson.mikael@gmail.com

Received 26 July 2013; Accepted 22 October 2013; Published 16 January 2014

Academic Editor: Haifeng Chen

Copyright © 2014 Mikael Larsson et al. This is an open access article distributed under the Creative Commons Attribution License, which permits unrestricted use, distribution, and reproduction in any medium, provided the original work is properly cited.

Biodegradable cell scaffolds and local drug delivery to stimulate cell response are currently receiving much scientific attention. Here we present a nanocomposite that combines biodegradation with controlled release of lithium, which is known to enhance bone growth. Nanogels of lithium neutralized polyacrylic acid were synthesized by microemulsion-templated polymerization and were incorporated into a biodegradable polyhydroxybutyrate (PHB) matrix. Nanogel size was characterized using dynamic light scattering, and the nanocomposites were characterized with regard to structure using scanning electron microscopy, mechanical properties using tensile testing, permeability using tritiated water, and lithium release in PBS using a lithium specific electrode. The nanogels were well dispersed in the composites and the mechanical properties were good, with a decrease in elastic modulus being compensated by increased tolerance to strain in the wet state. Approximately half of the lithium was released over about three hours, with the remaining fraction being trapped in the PHB for subsequent slow release during biodegradation. The prepared nanocomposites seem promising for use as dual functional scaffolds for bone regeneration. Here lithium ions were chosen as model drug, but the nanogels could potentially act as carriers for larger and more complex drugs, possibly while still carrying lithium.

1. Introduction

To introduce additional functionality in a biodegradable polyhydroxybutyrate (PHB) matrix, polyacrylic acid (PAA) nanogels were incorporated to form a hybrid solid-gel nanocomposite. This highly designed material structure approach is in line with recent developments in the biomaterials field.

Biodegradable materials have long been investigated for use in tissue engineering and drug delivery, as seen from literature [1–3], but attention has turned towards structured and/or multifunctional materials [3, 4]. One material class that has been widely investigated for use in biomedical applications is polyhydroxyalkanoates (PHA), as it incorporates a range of naturally occurring biocompatible aliphatic

polyesters, including PHB [5]. The characteristics and material properties of different PHA vary greatly, for example, mechanical properties and degradation rates can be tailored by the monomer composition [2, 3, 5]. When it comes to PHB it has a strong tendency for crystallization [5] and has a slow biodegradation rate compared to most biodegradable polyesters [6]. With regard to mechanical properties it is hard and brittle, where the brittleness is a disadvantage [5], and copolymers/composites may be better suited for biomedical applications [2, 5]. Nonetheless, PHB is generally nontoxic [5], likely because the polymer and its final degradation products are naturally occurring in humans [7, 8], and has been investigated for use in bone tissue engineering [2, 5, 9–11] and nerve scaffolding [12–14], among other applications. Recently there have been reports on creating nano-microporous PHB

matrixes using an aqueous emulsion as template for the voids in the material [6, 15].

PAA is an anionic polyelectrolyte that is easily polymerized and crosslinked into macroscopic hydrogels that can swell hundreds of times their dry weight, especially when the acid protons are neutralized with sodium [16]. PAA is a pharmaceutically used excipient also known under the name Carbopol [17]. There have been numerous studies on the use of PAA as a component in materials for biomedical applications, both because of its high swelling capability and because the polyanionic charge allows for easy loading of cationic molecules. In the last decade, there have been some reports on the preparation of PAA nanogels [18–20], and such nanogels have been investigated as drug carriers [18, 19]. Based on available literature on PHB, PAA nanogels, and other materials where nanodrug carriers have been incorporated in a macroscopic matrix [21–23], we recognized that if PAA nanogels could be synthesized and incorporated into PHB matrixes, then they could provide additional functionality to the materials by acting as drug carriers and possibly also altering the mechanical properties for beneficial effects. However, rather than incorporating conventional drugs into the PAA nanogels, as already proven possible, the very small monovalent cation lithium was chosen as a model substance. Lithium has been shown to activate the Wnt-signaling pathway [24, 25], leading to accumulation of β -catenin protein [25], a protein that in turn positively regulates osteoblasts [26], which clearly is of interest for bone-tissue engineering. In fact, lithium has been shown to increase bone mass and improve fracture healing in mice/rats [24, 26, 27]. Given the interest in PHB for bone-tissue regeneration lithium is a relevant choice as model drug; in addition, if controlled release is possible for lithium it will surely be possible for larger cationic drugs, especially if polyvalent.

In this study, we report on the successful preparation of drug loaded PHB-PAA nanogel composite films with designed structure, controlled release of lithium, and improved mechanical properties.

2. Materials and Methods

2.1. Materials. Acetone, acrylic acid anhydrous, chloroform puriss p.a, lithium hydroxide, N,N'-methylenebisacrylamid (MBA), poly-[(R)-3-hydroxybutyric acid] (PHB), polysorbate 80, poly[(R)-3-hydroxybutyric acid], potassium persulfate, Span 80, and N,N,N',N'-Tetramethylethylenediamine (TEMED) were purchased from Sigma Aldrich. Hexane was purchased from Fischer scientific. Milli-Q (Millipore) water was used throughout the experiments.

2.2. Preparation of Lithium Loaded PAA Nanogels by Reverse Microemulsion Polymerization. Adapted from work by others [18, 19], the following method was used for PAA nanogel preparation. In a vial 3.43 g Span 80 and 2.62 g Tween 80 were added, followed by 100 mL hexane (oil phase). The flask was capped and the content mixed with a magnetic stirrer so that tween and span were fully dissolved. The aqueous phase was prepared as follows: 1.5 mL of 10% (w/w) LiOH in H₂O

was added to 500 μ L acrylic acid. Subsequently, using H₂O as solvent, 214 μ L of 5% (w/v) MBA suspension, 500 μ L 2% (w/v) potassium persulfate, and 40 μ L of 20% (w/v) TEMED were added.

The microemulsion was formed by dropwise addition of the aqueous phase into the oil phase while a homogenizer (IKA, Taquara) was running at 14000 rpm. After the addition, the speed of the homogenizer was increased to 24000 rpm for 3 min, followed by 14000 rpm until all foam had disappeared (about 45 sec). The emulsion was transferred to a 60°C water bath and was stirred at 400 rpm using a magnetic stirrer. For the first 10 minutes the emulsion was covered with aluminum foil and bubbled with N₂, after which the vial was capped and the reaction was allowed to proceed for 6 h, after which the vial was vented, resealed, and left under stirring at room temperature overnight. For washing, product and solvent were transferred to 50 mL falcon tubes, and centrifuged at 5100 rpm for 6 h at 4°C using a Sigma 4kl5 centrifuge (Labex). The supernatants were decanted and the pellets were resuspended in acetone for a total volume of 20 mL and were centrifuged again at 5100 rpm for 10 min at 4°C, repeated three times. Finally, the pellets were re-suspended in acetone (final volume 5 mL) and mixed with magnetic stirrer overnight. The opaque dispersions were centrifuged down, the acetone was discarded, and the pellets were dispersed in 1 mL chloroform, pooled, and stored until further use and analysis.

2.3. Nanogel Size Characterization. Prior to washing samples were taken out and dispersed in H₂O. The dispersion was centrifuged, and the supernatant was diluted 100 times and filtered with a 0.20 μ m filter before analysis by dynamic light scattering (DLS) using a N4 plus submicron particle size analyzer (Beckman Coulter). The program was set to run at room temperature and measured all angles (5.7°, 11.1°, 23.0°, 30.2°, 62.6°, and 90.0°) for 6 min.

2.4. Film Preparation. Pure PHB films were prepared as follows: 560 mg PHB was dissolved in 8 mL chloroform under magnetic stirring in a 58°C water bath for 1 h. The solution was left to cool down to room temperature after which the PHB solution was poured in a glass petri dish. Film casting was performed by allowing the chloroform to evaporate without lid for 2 min before loosely covering the dish with a lid until the next day, at which point the evaporation was complete. To ensure an even evaporation, the glass petri dish had double layered tape on two edges.

PHB films containing PAA nanogels were prepared as above, with the following differences: PHB was dissolved in 6 mL chloroform, and the desired mass of PAA nanogels were mixed with 2 mL chloroform. The nanogel dispersion was then mixed with the PHB solution using a homogenizer (DII8, IKA) for 15 s, and casting was performed as for pure PHB films.

2.5. Film Structure Characterization. Dry films and freeze-dried (LABCONCO, FreeZone 6) swollen films were cut into sections to display the interior regions of the films. Before

the SEM analysis, all samples were sputter coated with gold in argon atmosphere for about 1 min using a S150B Sputter Coater (Edwards). SEM analysis was conducted using a LEO Ultra 55 SEM equipped with a field emission gun (LEO Electron Microscopy Group).

2.6. Swelling Analysis. Films were cut in 1.5×2 cm pieces. Dry weight and thickness of the pieces were recorded. The pieces were swollen in Milli-Q water or PBS buffer (pH 7.4). At pre-determined time times, excess water was removed by blotting the films on a paper and the weight and thickness of the samples were noted. The film pieces were then resubmerged. The swelling was calculated as

$$\text{Swelling degree (Q)} = \frac{W_s - W_d}{W_d}, \quad (1)$$

where W_s is the weight of the swollen sample and W_d is the dry weight.

2.7. Tensile Testing. Each film was cut into three rectangular strips using an 8.5 mm thick parallel cutter. The average thickness of each stripe was determined from three different sites. The films were mounted into the tensile tester (Instron) and were pulled until breakage while the force displacement was recorded.

2.8. Water Permeability. Film pieces were cut out, and the thickness was measured in triplicates and placed between the donor and acceptor compartment in diffusion cells. Subsequently, 50 mL of Milli-Q water was simultaneously added to the donor and acceptor compartments and $10 \mu\text{L}$ of tritiated water (400 kBq) was added to the donor compartments. During the experiment, the cells were placed on a rotating table for mixing at ambient temperature. At specified times $500 \mu\text{L}$ was extracted from the acceptor compartment and replaced with Milli-Q water. To determine the diffusive flow across the films, the tritium activity in the acceptor compartment was compared to the initial activity in the donor compartment using a liquid scintillation analyser (Tri-carb 2810 TR, Perkin Elmer). The permeability (P) of the films was calculated using the following equation:

$$\frac{2PS}{V}t = -\ln\left(\frac{C_{d,0} - 2C_a}{C_{d,0}}\right), \quad (2)$$

where S is the area through which diffusion occurs, V is the volume of the individual donor and acceptor compartments, t is the time, $C_{d,0}$ is the concentration in donor compartment at time zero, and C_a is the concentration in the acceptor compartment at time t . From a plot of $-\ln[(C_{d,0} - 2C_a)/C_{d,0}]$ versus time, P was calculated from the slope [28]. To eliminate contributions from film thickness (h), P was normalized by multiplication with h at time zero.

2.9. Lithium Release. PHB films containing 15 and 25% PAA were cut into 1.8×2 cm pieces that were subsequently immersed in 30 mL PBS buffer under stirring. At pre-determined times a calibrated ion specific electrode (ISE) for

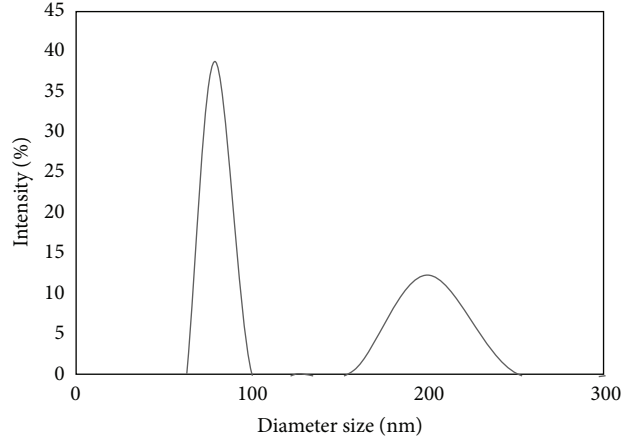


FIGURE 1: Exemplifying plot of intensity-size distribution for the nanogels in water.

TABLE 1: Average sizes and relative mass fraction, determined from DLS using the angle of 90° .

Diameter (nm)	Std. dev. (nm)	Relative mass fraction
79	5.4	3.3
200	13.7	1

lithium ions was used to measure the concentration of released lithium ions.

3. Results and Discussion

3.1. PAA Nanogel Synthesis and Characterization. Nanogels of PAA were prepared by reverse phase microemulsion polymerization. The model drug lithium was incorporated into the gels by neutralizing the carboxylic acid of the acrylic acid monomers prior to the polymerizations reaction. The condition of electroneutrality as well as the low chemical potential of lithium ions in the hydrophilic nanogels, compared to in the hydrophobic solvents used for washing, would lead to lithium remaining in the gels.

Analysis of the nanogels using DLS revealed two populations with different size, as shown in Figure 1. The average size of the two populations was about 80 nm and 200 nm, respectively. Similar results were obtained for all angles, indicating a spherical geometry of the nanogels.

From the intensity distribution the mass ratio between the two populations was calculated, recognizing that larger particles are given more weight in intensity distribution obtained from DLS. The calculations revealed that the mass fraction of nanogels in the population with smaller size was about three times the mass fraction in the population with larger size (see Table 1).

3.2. Casting of PHB-Nanogel Composite Films. Films of PHB with or without nanogels were prepared by solvent evaporation. All prepared films had thicknesses in the range of $95 \mu\text{m}$ – $150 \mu\text{m}$ and displayed a smooth surface. Pure PHB films were slightly opaque, and with increasing nanogel

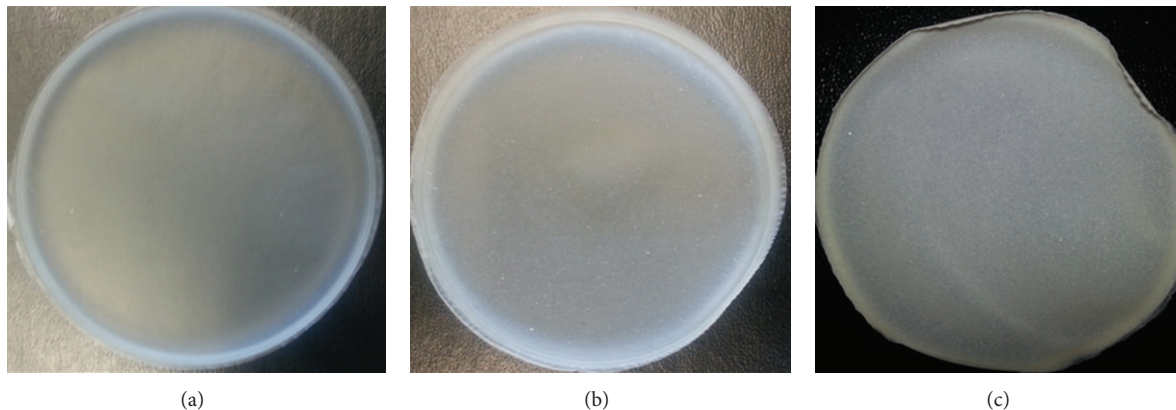


FIGURE 2: Photos of, (a) a PHB film, (b) PHB films containing 5% (w/w) PAA, and (c) PHB films containing 25% (w/w) PAA.

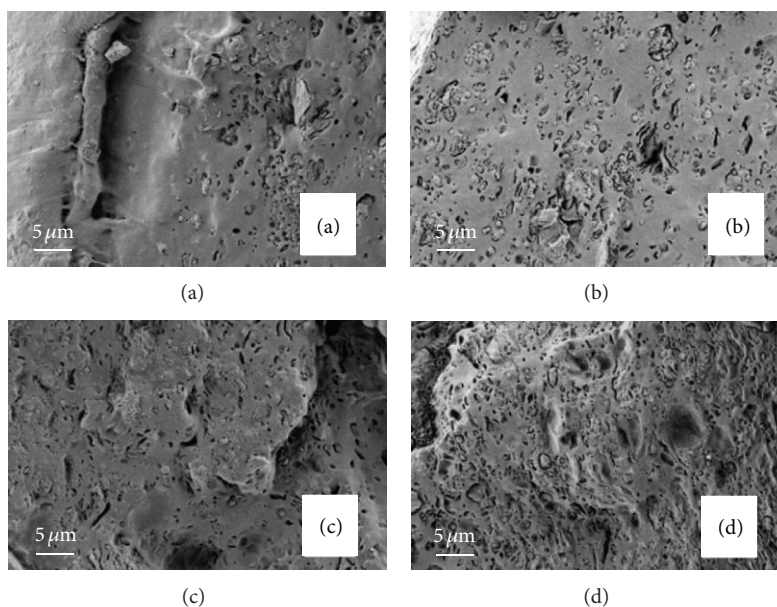


FIGURE 3: SEM micrographs showing the cross-sections of dry PHB films with different amounts of PAA nanogels: (a) PHB + 5% (w/w) PAA; (b) PHB + 10% (w/w) PAA; (c) PHB + 15% (w/w) PAA, and (d) PHB + 25% (w/w) PAA.

content the opaqueness increased, so that the films with 25% nanogels appeared close to white (Figure 2).

3.3. Morphology of the PHB-Nanogel Composite Films. To characterize the morphology of the formed nanocomposite films they were analysed using SEM. Analyses were performed both on dry films and on films swollen and subsequently freeze-dried. The dry films revealed an increasing porosity with increasing nanogel content (Figure 3).

For swollen and freeze-dried films, the trend of increasing porosity with increasing nanogel content was even more pronounced (Figure 4), not surprising given that the PAA nanogels should swell in water and delocalize the surrounding PHB to some extent. Upon freeze drying the changed structure should remain to large parts. In summary, the nanogels were well dispersed throughout the nano-composite, induced

a more porous structure, and swelled in water to further increase the porosity of the PHB matrix.

3.4. Swelling and Water Permeability of the PHB-Nanogel Composite Films. Swelling and permeability are both of relevance for biomedical applications. The swelling influences mechanical properties and mass transfer in the material, while permeability is a measurement of how easy molecules can be transported through the material.

In PBS pure PHB films displayed little swelling, but the swelling increased with increasing nanogel content. A large increase in swelling (per mass nanogel) was seen for the samples with the lowest nanogel content (5%), followed by smaller increase with additional nanogel addition (Figure 5(a)). The trend was similar for swelling in Milli-Q water but with some notable differences. The swelling of pure PHB

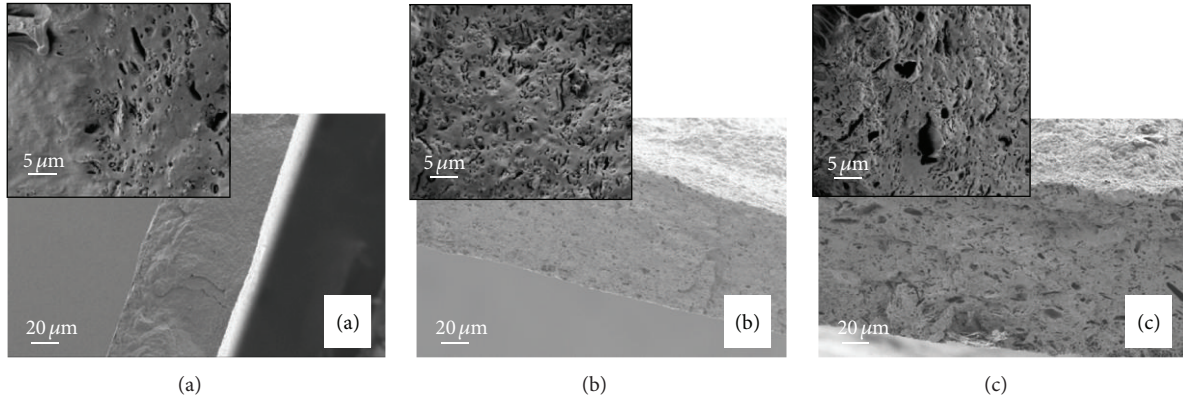


FIGURE 4: SEM micrographs showing the cross-sections of swollen and subsequently freeze-dried PHB films with different PAA nanogel content: (a) PHB; (b) PHB + 15% (w/w) PAA; (c) PHB + 25% (w/w) PAA.

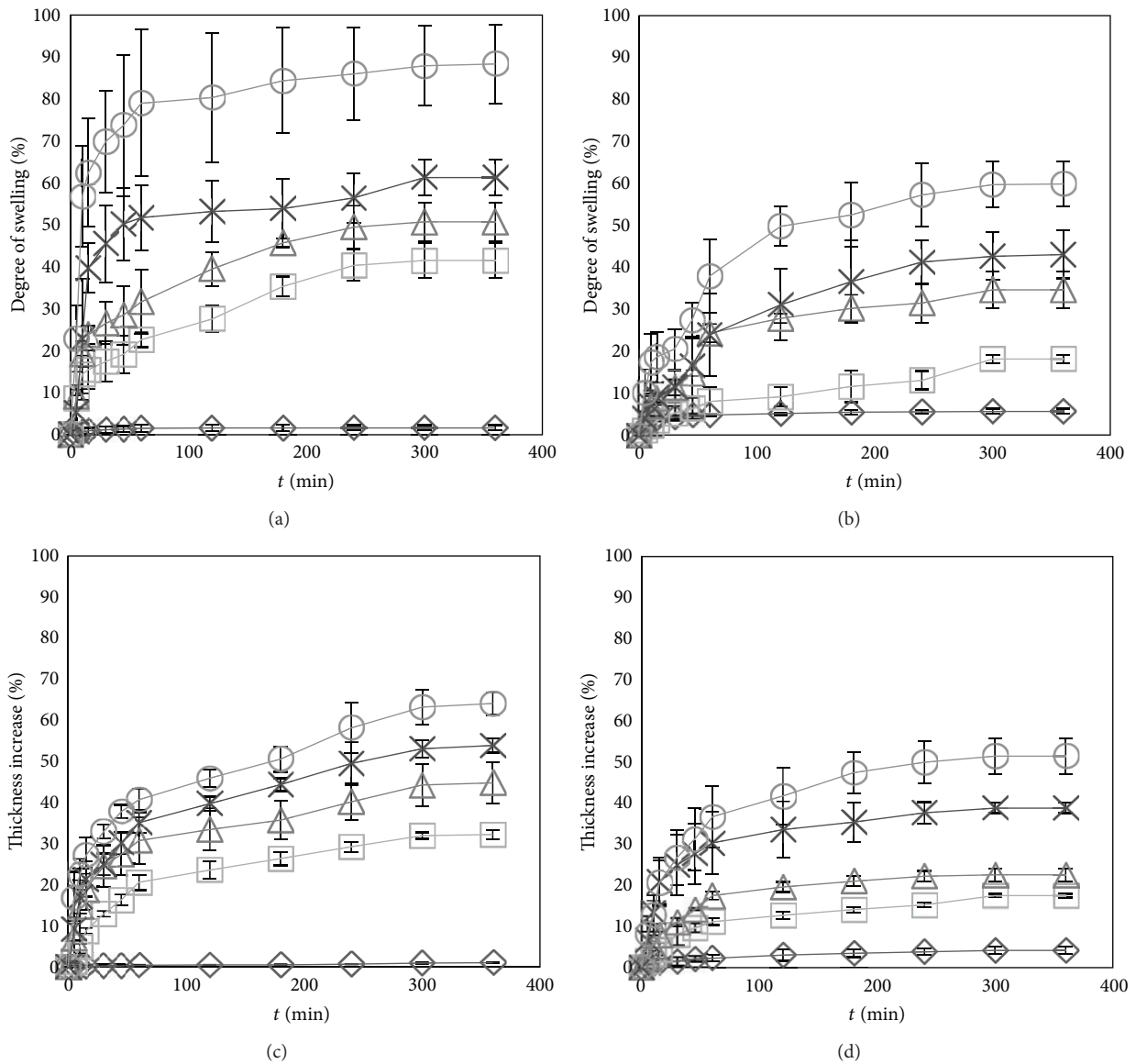


FIGURE 5: Swelling behavior of PHB films with different PAA nanogel content. (a) % mass increase in PBS buffer, (b) % mass increase in Milli-Q water, (c) % thickness increase in PBS buffer, and (d) % thickness increase in Milli-Q water. \diamond = PHB, \square = PHB + 5% PAA, Δ = PHB + 10% PAA, \times = PHB + 15% PAA, \circ = PHB + 25% PAA. Error bars indicate one standard deviation ($n = 3$).

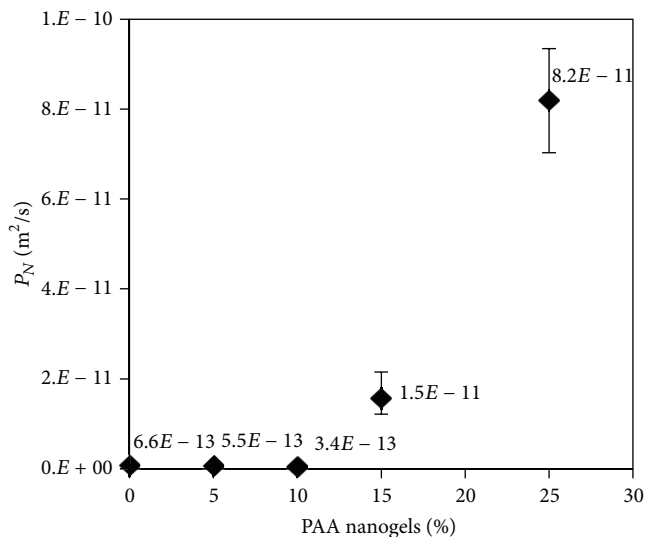


FIGURE 6: Water permeability normalized for initial film thickness for PHB films with different PAA nanogel content. Error bars indicate min/max ($n = 2-5$).

was somewhat increased in Milli-Q water, while the swelling of the composites was reduced for all nanogel contents (Figure 5(b)). To elucidate the dimensional changes upon swelling the thickness of swollen samples was measured in addition to weight. It was found that most of the swelling occurred by increasing the thickness of the samples (Figures 5(c) and 5(d)). The exact mechanisms behind the observed swelling, behaviours may be complex and merit further investigation before conclusions are drawn. However, what can be stated is that the nanogels increased the swelling of the composite and that they should exist in a swollen gel state inside submerged composites. Furthermore, since the thickness of PHB increased upon submersion in PBS the PHB did indeed swell; that is, the increase in mass was not only due to water becoming trapped in cracks and pores.

It is well known that for polymer materials the diffusion coefficient quickly increases with swelling of the material [29] and that in a composite combining regions with small and large diffusion coefficients the spatial distribution of those will influence the permeability [30]. Therefore, permeability analysis was conducted on pure PHB films and the composites. Very low permeability was observed for pure PHB films and composites with 5% and 10% nanogels, while for films with higher (15% and 25%) nanogel content the permeability increased rapidly (Figure 6). The results are explained as follows: the diffusion is slow in PHB, while it is fast in the swollen nanogels. Below a critical nanogel content there is no connectivity between them and the permeability is limited by diffusion through PHB. However, at higher nanogel concentrations they form a coherent network that percolates through the films, effectively creating channels with large diffusion coefficient, with increased permeability as a consequence. The results are in agreement with those from the SEM analysis and are highly relevant for predicting drug release behaviour of the PHB-nanogel composites. For

composites with $\leq 10\%$ nanogels drug release would likely be controlled by degradation of the PHB, while for higher nanogel content at least a fraction of the loaded drug would be released faster through diffusion.

3.5. Release of Lithium from the PHB-Nanogel Composite Films. Having established the structure and permeability of the PHB-nanogel composites, the release of lithium was investigated for nanogel contents of 15% and 25%. Composites with lower nanogel content were excluded as the permeability analysis had revealed them to only allow for very limited diffusion through them. Worth mentioning is that *in vivo* the composites with very low permeability should release nanogels and loaded drugs as the PHB degrade.

Both the composites with 15% and 25% nanogels displayed a close to linear release of lithium during the first 1.5 h, after which the drug release levelled off. At the final measuring time of 7 h the percent of lithium released from the gels was 41% and 58% for nanogel contents of 15% and 25%, respectively (Figure 7). The fact that the drug release is far from 100% indicates that a fraction of the nanogels are not part of the percolating network; thus, the release of lithium from this fraction is extremely slow, so that only the release of lithium in the percolating nanogel fraction is detected. The observation that a higher percent of lithium was released from the composites with higher nanogel content is coherent with that the fraction of nanogels belonging to the percolating network increases with nanogel content, as expected. The lithium release profiles indicate that the prepared PHB-nanogel composites can be loaded with drug for controlled diffusive release of active agents, if the nanogel content is high enough. At lower nanogel content the release will instead be determined by PHB degradation. If desired it should be possible to achieve a combination of fast diffusion controlled release and slow degradation controlled release by choosing suitable nanogel content.

3.6. Mechanical Properties of the PHB-Nanogel Composite Films. Even if PHB has been investigated with promising results for bone-tissue regeneration, it has been stated that its brittleness may limit the use of pure PHB in therapeutic applications [2, 5]. Recognizing the importance of mechanical properties in biomedical applications the PHB-nanogel composite films were analysed using tensile testing in the dry and equilibrium swollen state. With increasing nanogel content the elastic modulus (E) decreased from 1.4 GPa to 0.7 GPa and from 1 GPa to 0.5 GPa for dry and equilibrium swollen samples, respectively (Figure 8(a)). The decrease in E with nanogel addition was expected, especially in the wet state where E of the nanogel phase is very low. With regard to tolerance to extension (the percent extension at which breakage occurred) there was no conclusive effect of nanogel content for the dry samples. However, for equilibrium swollen samples tolerance to extension surprisingly increased (Figure 8(b)). This improvement in extension properties suggests that the wet nanogels interact with the PHB on a molecular level, causing plasticizing of the material.

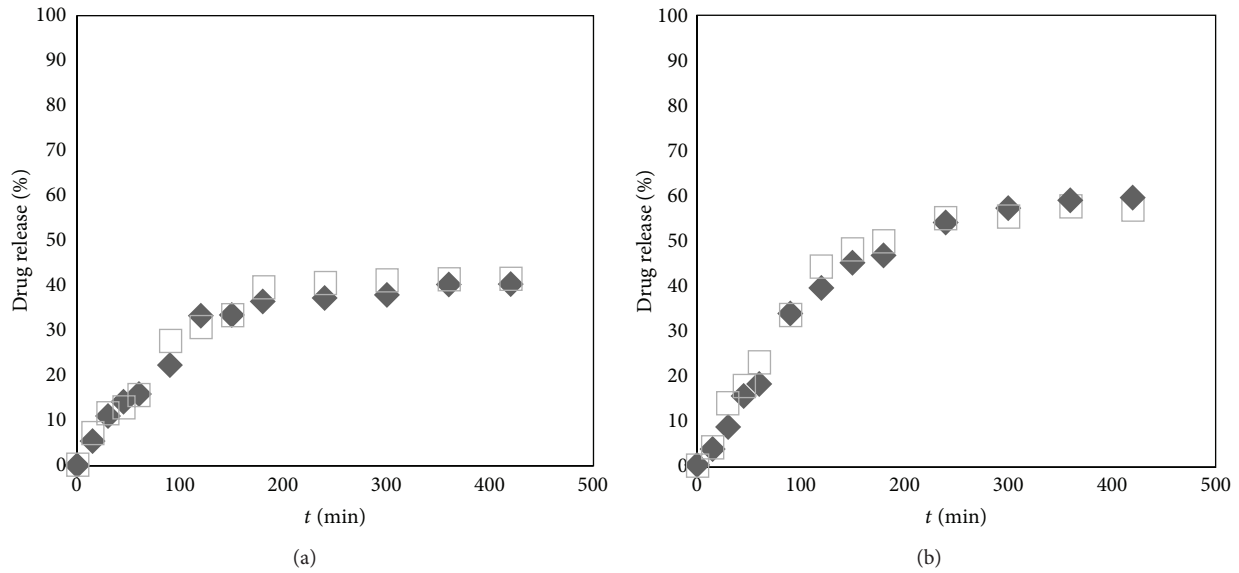


FIGURE 7: Release of lithium ions from PHB-nanogel composite films in PBS. (a) 15% (w/w) nanogels, (b) 25% (w/w) nanogels. The different markers indicate two independent experiments.

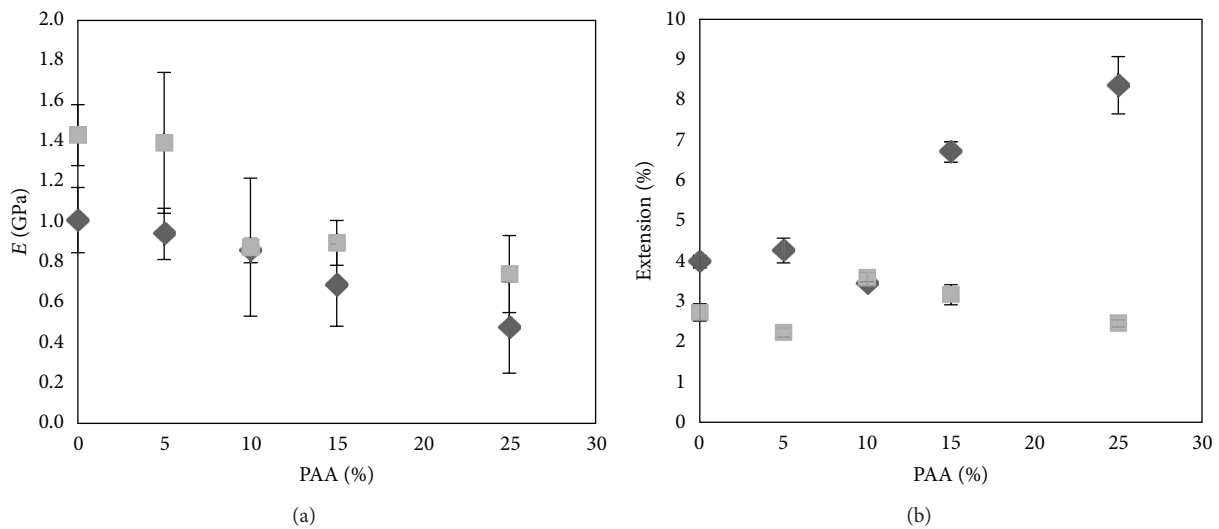


FIGURE 8: (a) Elastic modulus and (b) extension at breakage for dry (\square) and swollen (\diamond) PHB films with different PAA nanogel content. Error bars indicate one standard deviation ($n = 3$).

The results from the tensile testing revealed that the PHB-nanogel composites retained a high elastic modulus, even if decreased to about half. More importantly the composites seem to overcome the limitation of the inherent brittleness of PHB, making the composites highly interesting for therapeutic uses.

4. Conclusion

Composite films composed of PHB and PAA nanogels were prepared and characterized. The results indicate that the composites may be well suitable for biomedical uses as a biodegradable material where nanostructural design may be

used to tune drug release mechanism, from diffusion controlled to degradation controlled. Furthermore, controlled release was demonstrated for the small lithium ion which together with improved tolerance to deformation suggest the nanocomposites to be suitable for bone-tissue engineering. Lithium is a relevant therapeutic substance in itself, but even more, the fact that controlled release is achieved for the small monovalent lithium ion clearly indicates potential for delivery of more complex substances. Further investigations involving the material would involve both fundamental investigations of the mechanisms behind swelling behaviour and mechanical properties, as well as applied *in vivo* studies using lithium and other therapeutic substances.

Conflict of Interests

The authors declare that there is no conflict of interests regarding the publication of this paper.

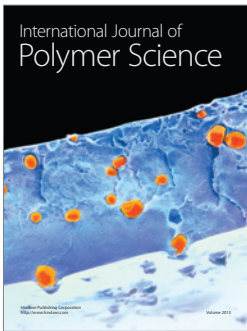
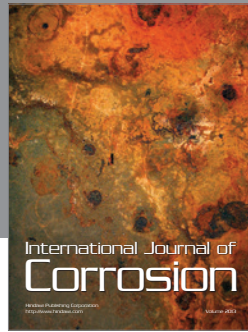
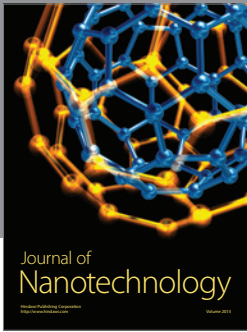
Acknowledgments

This project was part of the VINN Excellence Centre SuMo Biomaterials (Supermolecular Biomaterials-Structure dynamics and properties). The financial support from the centre is gratefully acknowledged. Further financial support was acquired from the Swedish Research Council and from the Chalmers Bioscience Program, Chalmers University of Technology. Many thanks are due to Anders Mårtensson and Dr. Romain Bordes (Chalmers University of Technology) for assistance with SEM and DLS analyses.

References

- [1] M. Chasin and R. Langer, Eds., *Biodegradable Polymers as Drug Delivery Systems*, Marcel Dekker, New York, NY, USA, 1990.
- [2] M. I. Sabir, X. Xu, and L. Li, "A review on biodegradable polymeric materials for bone tissue engineering applications," *Journal of Materials Science*, vol. 44, no. 21, pp. 5713–5724, 2009.
- [3] Y. Yang and A. J. El Haj, "Biodegradable scaffolds—delivery systems for cell therapies," *Expert Opinion on Biological Therapy*, vol. 6, no. 5, pp. 485–498, 2006.
- [4] M. Larsson, W. C. Huang, M. H. Hsiao et al., "Biomedical applications and colloidal properties of amphiphilically modified chitosan hybrids," *Progress in Polymer Science*, vol. 38, no. 9, pp. 1307–1328, 2013.
- [5] S. K. Misra, S. P. Valappil, I. Roy, and A. R. Boccaccini, "Polyhydroxyalkanoate (PHA)/inorganic phase composites for tissue engineering applications," *Biomacromolecules*, vol. 7, no. 8, pp. 2249–2258, 2006.
- [6] A. Bergstrand, H. Andersson, J. Cramby, K. Sott, and A. Larsson, "Preparation of porous poly(3-Hydroxybutyrate) films by water-droplet templating," *Journal of Biomaterials and Nanobiotechnology*, vol. 3, no. 4, pp. 431–439, 2012.
- [7] R. N. Reusch, A. W. Sparrow, and J. Gardiner, "Transport of poly- β -hydroxybutyrate in human plasma," *Biochimica et Biophysica Acta*, vol. 1123, no. 1, pp. 33–40, 1992.
- [8] T. Saito, K. Tomita, K. Juni, and K. Ooba, "In vivo and in vitro degradation of poly(3-hydroxybutyrate) in rat," *Biomaterials*, vol. 12, no. 3, pp. 309–312, 1991.
- [9] C. Doyle, E. T. Tanner, and W. Bonfield, "In vitro and in vivo evaluation of polyhydroxybutyrate and of polyhydroxybutyrate reinforced with hydroxyapatite," *Biomaterials*, vol. 12, no. 9, pp. 841–847, 1991.
- [10] A. Zonari, S. Novikoff, N. R. P. Electo et al., "Endothelial differentiation of human stem cells seeded onto electrospun polyhydroxybutyrate/polyhydroxybutyrate-co-hydroxyvalerate fiber mesh," *PLoS ONE*, vol. 7, no. 4, Article ID e35422, 2012.
- [11] E. C. Carlo, A. P. B. Borges, R. J. Del Carlo et al., "Comparison of in vivo properties of hydroxyapatite-polyhydroxybutyrate composites assessed for bone substitution," *Journal of Craniofacial Surgery*, vol. 20, no. 3, pp. 853–859, 2009.
- [12] P.-N. Mohanna, R. C. Young, M. Wiberg, and G. Terenghi, "A composite pol-hydroxybutyrate-glia growth factor conduit for long nerve gap repairs," *Journal of Anatomy*, vol. 203, no. 6, pp. 553–565, 2003.
- [13] M. Åberg, C. Ljungberg, E. Edin et al., "Clinical evaluation of a resorbable wrap-around implant as an alternative to nerve repair: a prospective, assessor-blinded, randomised clinical study of sensory, motor and functional recovery after peripheral nerve repair," *Journal of Plastic, Reconstructive and Aesthetic Surgery*, vol. 62, no. 11, pp. 1503–1509, 2009.
- [14] M. T. Khorasani, S. A. Mirmohammadi, and S. Irani, "Polyhydroxybutyrate (PHB) scaffolds as a model for nerve tissue engineering application: fabrication and in vitro assay," *International Journal of Polymeric Materials*, vol. 60, no. 8, pp. 562–575, 2011.
- [15] C. Zhijiang, "Biocompatibility and biodegradation of novel PHB porous substrates with controlled multi-pore size by emulsion templates method," *Journal of Materials Science*, vol. 17, no. 12, pp. 1297–1303, 2006.
- [16] M. Larsson, S. Gustafsson, E. Olsson, and A. Larsson, "Effect of calcium neutralization on elastic and swelling properties of crosslinked poly(acrylic acid)—correlation to inhomogeneities and phase behaviour," *e-Polymers*, vol. 9, no. 1, pp. 1683–1696, 2013.
- [17] R. C. Rowe, P. J. Sheskey, and M. E. Quinn, Eds., *Handbook of Pharmaceutical Excipients*, Pharmaceutical Press and American Pharmacist Association, Chicago, Ill, USA, 6th edition, 2009.
- [18] T. K. De and A. S. Hoffman, "An ophthalmic formulation of a beta-adrenoceptor antagonist, levobetaxolol, using poly(acrylic acid) nanoparticles as carrier: loading and release studies," *Journal of Bioactive and Compatible Polymers*, vol. 16, no. 1, pp. 20–31, 2001.
- [19] T. K. De and A. S. Hoffman, "A reverse microemulsion polymerization method for preparation of bioadhesive polyacrylic acid nanoparticles for mucosal drug delivery: loading and release of timolol maleate," *Artificial Cells, Blood Substitutes, and Immobilization Biotechnology*, vol. 29, no. 1, pp. 31–46, 2001.
- [20] R. Melinda Molnar, M. Bodnar, J. F. Hartmann, and J. Borbely, "Preparation and characterization of poly(acrylic acid)-based nanoparticles," *Colloid and Polymer Science*, vol. 287, no. 6, pp. 739–744, 2009.
- [21] M. H. Hsiao, M. Larsson, A. Larsson et al., "Design and characterization of a novel amphiphilic chitosan nanocapsule-based thermo-gelling biogel with sustained in vivo release of the hydrophilic anti-epilepsy drug ethosuximide," *Journal of Controlled Release*, vol. 161, no. 3, pp. 942–948, 2012.
- [22] L.-J. Lin, M. Larsson, and D.-M. Liu, "A novel dual-structure, self-healable, polysaccharide based hybrid nanogel for biomedical uses," *Soft Matter*, vol. 7, no. 12, pp. 5816–5825, 2011.
- [23] L. Zhao, L. Zhu, F. Liu et al., "pH triggered injectable amphiphilic hydrogel containing doxorubicin and paclitaxel," *International Journal of Pharmaceutics*, vol. 410, no. 1–2, pp. 83–91, 2011.
- [24] P. Clément-Lacroix, M. Ai, F. Morvan et al., "Lrp5-independent activation of Wnt signaling by lithium chloride increases bone formation and bone mass in mice," *Proceedings of the National Academy of Sciences of the United States of America*, vol. 102, no. 48, pp. 17406–17411, 2005.
- [25] C. M. Hedgepeth, L. J. Conrad, J. Zhang, H.-C. Huang, V. M. Y. Lee, and P. S. Klein, "Activation of the Wnt signaling pathway: a molecular mechanism for lithium action," *Developmental Biology*, vol. 185, no. 1, pp. 82–91, 1997.
- [26] Y. Chen, H. C. Whetstone, A. C. Lin et al., "Beta-catenin signaling plays a disparate role in different phases of fracture repair: implications for therapy to improve bone healing," *PLoS Medicine*, vol. 4, no. 7, article e249, 2007.

- [27] F. Kugimiya, H. Kawaguchi, S. Ohba et al., "GSK-3 β controls osteogenesis through regulating Runx2 activity," *PLoS ONE*, vol. 2, no. 9, article e837, 2007.
- [28] G. Van den Mooter, C. Samyn, and R. Kinget, "Characterization of colon-specific azo polymers: a study of the swelling properties and the permeability of isolated polymer films," *International Journal of Pharmaceutics*, vol. 111, no. 2, pp. 127–136, 1994.
- [29] L. Masaro and X. X. Zhu, "Physical models of diffusion for polymer solutions, gels and solids," *Progress in Polymer Science*, vol. 24, no. 5, pp. 731–775, 1999.
- [30] M. Larsson, J. Hjártstam, and A. Larsson, "Novel nanostructured microfibrillated cellulose-hydroxypropyl methylcellulose films with large one-dimensional swelling and tunable permeability," *Carbohydrate Polymers*, vol. 88, no. 2, pp. 763–771, 2012.



Hindawi

Submit your manuscripts at
<http://www.hindawi.com>

